A Wearable All-Printed Textile-Based 6.78 MHz 15 W-Output Wireless Power Transfer System and its Screen-Printed Joule Heater Application

Mahmoud Wagih, *Member, IEEE*, Abiodun Komolafe, *Member, IEEE*,
Alex S. Weddell, *Member, IEEE*, and Steve Beeby, *Fellow, IEEE*

***Abstract*—While research in passive flexible circuits for Wireless Power Transfer (WPT) such as coils and resonators continues to advance, limitations in their power handling and low efficiency have hindered the realization of efficient all-printed high-power wearable WPT receivers. Here, we propose a screen-printed textile-based 6.78 MHz resonant inductive WPT system using planar inductors with concealed metal-insulator-metal (MIM) tuning capacitors. A printed voltage doubler rectifier based on Silicon Carbide (SiC) diodes is designed and integrated with the coils, showing a power conversion efficiency of 80-90% for inputs between 2 and 40 W. Compared to prior wearable WPT receivers, it offers an order of magnitude improvement in power handling along with higher efficiency (approaching 60%), while using all-printed passives and a compact rectifier. The coils exhibit a simulated Specific Absorption Rate (SAR) under 0.4 W/kg for 25 W received power, and under 21°C increase in the coils' temperature for a 15 W DC output. We finally demonstrate a wirelessly-powered textile-based carbon-silver Joule heater, capable of reaching up to 60°C at 2 cm separation from the transmitter, as a potential wearable application which can only be wireless-powered using the proposed system.**

***Index Terms*—Antennas, Coils, Heaters, Inductors, Rectifiers, Resistors, RFID, Wireless Power Transfer.**

I. Introduction

FLEXIBLE wearable systems represent the closest sensing and actuation platform to the user [1]. Emerging wearable sensing systems [2]–[4], antennas [5], and body area networks [6] have mostly been implemented using flexible or textile-based materials, for seamless integration into clothing. It is widely recognized that conventional batteries are not a wearable-friendly option [7]–[9], leading to research efforts seeking a solution in wireless power transfer (WPT) [9]–[11] and in flexible or wearable energy harvesters [7], [12].

While low-power wearable sensors can be powered using far/mid-field WPT [13], wearable applications such as Joule heaters [14] or mobile neural network classification processors, sampling wearable sensors [15], cannot be powered using any of the reported wearable textile-based energy harvesting or WPT solutions. To explain, wearable mid/far-field WPT solutions are focused on μW to mW applications [9], [16], [17]. Moreover, wearable and implantable near-field WPT research is mostly focused on the passive electromagnetic link [11], [18]–[20], with no flexible or textile-based rectifiers designed and optimized for wearable or large-area electronics.

Individual additively-manufactured passive components, however, show promise for all-printed WPT receivers. For example, inkjet printed RLC circuits have been reported on smooth thin films, handling around 100 mW [21]. Furthermore, printed capacitors on rough textile substrates have recently been demonstrated with better microwave power-handling (up to 1 W) than their discrete ceramic counterparts [22]. Printed textile-based coils were integrated with rigid FR4-based Qi-standard circuitry in [23] and demonstrated receiving around 1.5 W with a 37% DC-DC efficiency. In [24], we demonstrated a 3.75 W 6.78 MHz WPT receiver based on a flexible rectifier and resonant embroidered coils. However the WPT system in [24] had several limitations which cannot be solved using existing flexible and wearable WPT implementations including: (a) low power-handling capability of compact (<1 cm) surface-mount tuning capacitors, (b) low efficiency of the rectifier due to the high switching speed and the small form-factor, (c) high thermal losses with a peak temperature exceeding 150°C, and (d) unreliable packaging due to using multiple fabrication processes (embroidered coils, copper-based rectifier), and the surface mismatch caused by the flexible-rigid interface between the tuning rigid capacitors and the coils. Therefore, there has been no work to date demonstrating the feasibility of efficient (>50%) and high-power (>3 W) WPT using all-flexible resonators and power conversion circuits.

In this paper, we propose a printed textile-based wirelessly-powered system which addresses the outstanding challenge of high-power wearable WPT, that is the realization of an all-flexible WPT receiver. First, the design and fabrication of

Manuscript received Month xx, 2xxx; revised Month xx, xxxx; accepted Month x, xxxx. This work was supported by the UK Engineering and Physical Sciences Research Council (EPSRC) under Grant EP/P010164/1, the European Commission through the EnABLES Project grant number: 730957. The work of M. Wagih was supported by the UK Royal Academy of Engineering (RAEng) and the Office of the Chief Science Adviser for National Security under the UK Intelligence Community Post-Doctoral Research Fellowship programme. The work of S. Beeby was supported by the RAEng under the Chairs in Emerging Technologies scheme. (*Corresponding author: Mahmoud Wagih*).

M. Wagih is with the James Watt School of Engineering, the University of Glasgow, Glasgow, G12 8QQ, U.K. (phone: +44 0141 330 5042, email: mahmoud.wagih@glasgow.ac.uk).

A. Komolafe, A. S. Weddell, and S. Beeby are with the School of Electronics and Computer science, University of Southampton, Southampton, SO17 1BJ, U.K. (email: aok1g15; asw; spb@ecs.soton.ac.uk)

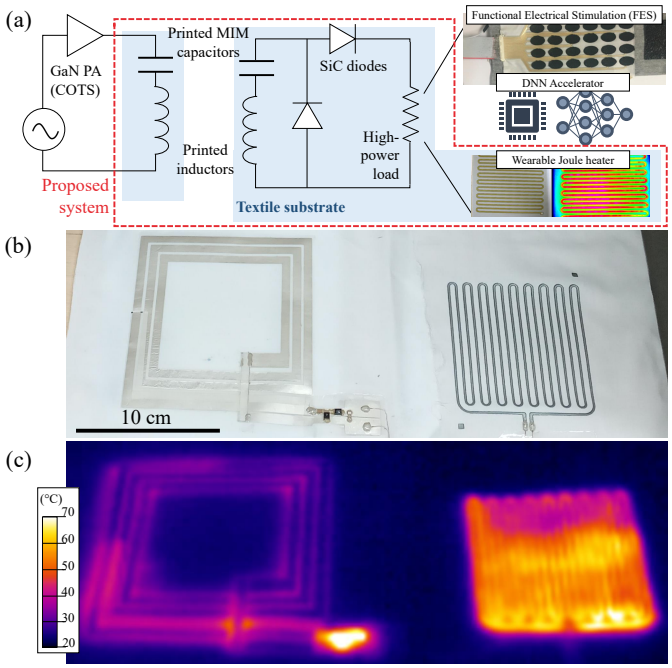

Fig. 1. (a) Schematic of the proposed high-power wearable WPT system and examples of its power-hungry wearable applications [25]; (b) photograph of the integrated system; (c) thermal image showing the heater's operation.

screen-printable resonant coils, suitable for integration on any textile substrate is presented (Section II), achieving up to 70% link efficiency (Section III). The coils are integrated with a flexible textile-based >90%-efficient voltage doubler, using off-the-shelf diodes, receiving over 14 W with an end-to-end efficiency of 60% (Section IV-A and B), and is demonstrated powering a printed heater with over 2 cm range (Section IV-C).

II. All-Printed Coils Design and Fabrication

To enable textile-integrated WPT to supply high-power wearable applications, such as the Joule heater presented here, the system illustrated in Fig. 1 is proposed. A typical printed e-textile heater consumes over 1 W of DC power [14], implying that existing wearable WPT systems cannot power these directly and must instead charge a battery which in turn periodically supplies the textile heater.

The coils and their tuning capacitors are realized using an inexpensive screen printing and lamination process, detailed in the next section, enabling them to achieve higher power handling than prior work utilizing discrete components [24]. The rectifier is seamlessly integrated on the same textile substrate and encapsulated for mechanical reliability. Both textile-based and conventional transmitter coils are characterized, using small-signal s-parameters, investigating the potential for WPT transmitters being integrated in non-wearable and industrial textiles used in furnishings (e.g.s chairs). Fig. 1(b) and (c) show the complete system being wirelessly-powered using a textile-based transmitting coil, placed beneath the visible coil in the photograph, driven by a Commercial-Off-The-Shelf (COTS) GaN power amplifier (PA) demonstration kit (GSWP050W-EVBPA).

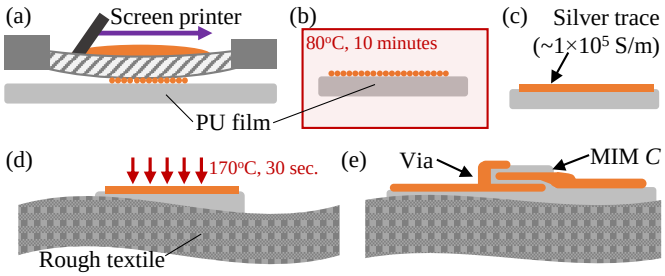

Fig. 2. Fabrication steps of the textile-based coils: (a) printing the conductors on the transfer layer; (b) initial curing; (c) the dried silver adhesive (PU)-backed film; (d) heat-transfer onto a textile substrate ; (e) the assembled structure.

A. Fabrication Method and Material Characterization

Instead of directly screen printing on the substrate, e.g. rough fabrics, the conductors are printed on a smooth 75 µm-thick polyurethane (PU) film, which is then heat-pressed onto the fabric, as in Fig. 2(a) to (d). To explain, fabric typically requires blanket coated textiles or the prior screen printing of specialist interface layers [26], and can limit curing temperatures. We have previously shown that by printing on the PU film, the printed traces can withstand over 10,000 bending cycles and can be applied to different textiles regardless of their roughness [22].

By laminating multiple PU/silver layers onto the textile, metal-insulator-metal (MIM) capacitors can be realized, as in Fig. 2(e), which can be used to tune the coils. These capacitors exhibit improved mechanical reliability over their inkjet counterparts [21], [27], which are restricted to smooth polymers and thin conductors. The large-area printed capacitors can achieve higher power handling than discrete ceramic capacitors. Once the circuit is printed, the components are attached using conductive epoxy, cured at 90°C, then encapsulated using a PU superstrate for mechanical reliability.

To realize tuning capacitors C for inductive or resonant WPT, C is given by

$$C = \frac{1}{4\pi^2 f_r^2 L} = \epsilon_{\mathrm{PU}} \frac{W_c L_c}{t} \tag{1}$$

where f_r=6.78 MHz, ϵ_{PU} is the permittivity of the PU film at 6.78 MHz, in Fig. 3, t=55 µm, the measured height of the heat-pressed dielectric, with L_c and W_c representing the length and width of the integrated tuning capacitor, respectively, as shown in Fig. 4(a).

The relative permittivity of the heat-pressed PU laminates was measured using a test MIM capacitor of known dimensions. The capacitance was measured using a Wayne Kerr 6500 impedance analyzer between 100 Hz and 10 MHz, which is lower than the capacitor's self-resonant frequency (SRF). Fig. 3 shows the calculated $\Re\{\epsilon_r\}$ of the PU laminate, where it can be seen that the PU maintains $\Re\{\epsilon_r\}$=2.4 at 6.78 MHz.

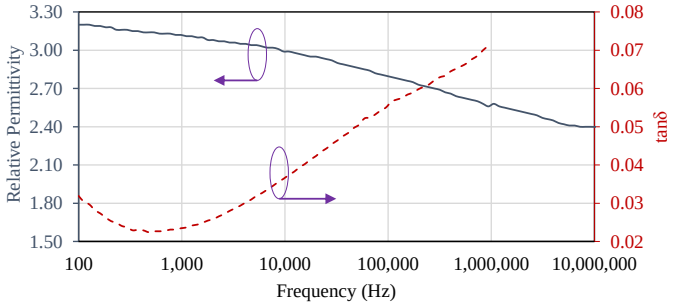

Fig. 3. Measured real relative permittivity and tanδ of the 55 µm-thick pressed PU with silver conductors.

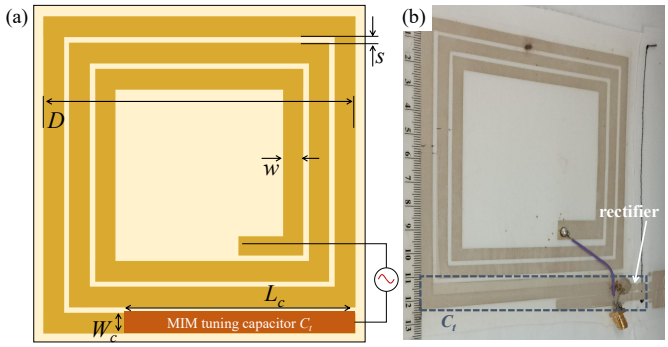

Fig. 4. (a) Generic layout of the coils showing the key dimensions; (b) photograph of coil A.

TABLE I
SUMMARY OF THE COILS' PARAMETERS

Coil	Calc. L (µH)	Meas. L, 6.78 MHz	Meas. R, 6.78 MHz	w (mm)	s (mm)	D (mm)	n
A	1.40	1.41 µH	15.3 Ω	10	2.5	150	3
B	1.71	1.48 µH	20.2 Ω	5	2.5	120	3
C	1.98	1.74 µH	20.4 Ω	2.5	2.5	105	3
D	0.62	0.72 µH	11.1 Ω	2.5	2.5	50	5

B. Coil, Capacitor, and Rectifier Design

Four square coils of varying sizes were designed. The inductance of the coils was approximated using the modifier Wheeler formula by Mohan *et al.* for printed inductors [28]. The uniform square geometry was chosen due to its simple closed-form analysis and its wide adoption in flexible and printed electronics [29]. Table I summarizes the geometrical and electrical parameters of each coil, along with their measured inductance; the layout of a 3-turn (n=3) coil is shown in Fig. 4(a), where the laminated capacitor can be observed.

Along with the printed coils and tuning capacitors, a flexible textile-based rectifier is integrated on the same substrate. The rectifier is a voltage doubler based on a Silicon Carbide (SiC) Schottky diode (GB01SLT12-214), chosen for its high reverse breakdown voltage of 1.2 kV, and low total capacitance of 71 pF, which enables a high RF to DC power conversion efficiency (PCE) and low thermal losses. A voltage doubler topology was chosen to enable a high voltage output which could, for example, directly power a wearable heater (as detailed later) without DC-DC conversion, as well as to reduce the component count, lowering the packaging and layout complexity as well as overall cost. The simulated and measured DC output of the rectifier is presented in Section IV-A-A.

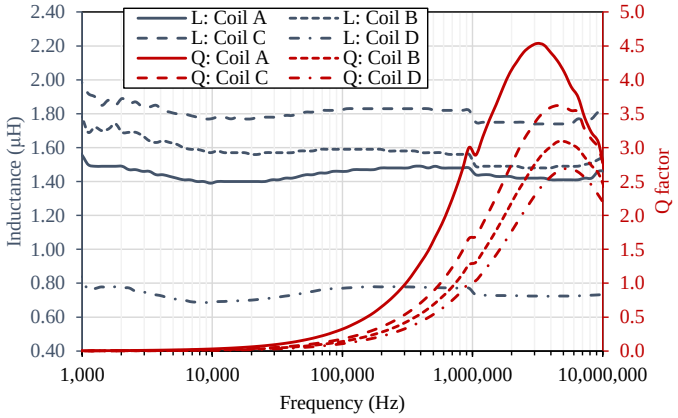

Fig. 5. Measured broadband inductance and Q-factor of the printed coils before integrating the tuning capacitors.

III. SMALL-SIGNAL COIL AND LINK CHARACTERIZATION

The coil parameters were measured using the impedance analyzer from 1 KHz to 10 MHz, and are shown in Fig. 5. The coil parameters are compared to the analytical L in Table I. A Rohde & Schwarz ZVB4 Vector Network Analyzer (VNA) was used to measure the s-parameters of the coils under varying separation and misalignment. SMA connectors were added to the resonant coils with the concealed capacitors to interface with the VNA, as shown in Fig. 4(b). The measured Q-factor (under 5 around 6.78 MHz) is comparable to previously reported printed coils implemented on smooth films [21], [30], showing that printing on the PU first and then laminating on to the textile does not affect coil properties.

The s-parameters of the one-to-one link, based on the printed coils, were simulated in CST Microwave Studio and measured using the VNA. Fig. 6 shows the simulated and measured s-parameters of the one-to-one link based on coils A and C, in close agreement. The conductivity of the coils was modelled as σ=1×10^4 S/m. From the S_{11} response, it can be seen that the coils are highly-coupled for separations under 2 cm, which is attributed to their relatively low inductance.

The s-parameters of the printed WPT coils were then characterized with a standard wire coil representing a non-textile transmitter. The coil is fabricated using a low-loss Litz wire, to act as a reference transmitter coil. The wire coil is composed of 5 turns, D=15 cm and has an inductance of 5.2 µH inductance, and 70 mΩ series resistance at 6.78 MHz. The forward transmission (S_{21}) between textile-based coils and the Litz coil was characterized for varying vertical separation as well as lateral misalignment. Fig. 7 shows the measured S_{21} as a function of vertical separation. To investigate the influence of the printed capacitor on the link, the s-parameters of coil C were also measured with a discrete ceramic tuning capacitor alongside the printed capacitor.

From Fig. 7, it can be seen that there is minimal influence on the S_{21} from using the printed capacitor. Moreover, the S_{21} variation with vertical separation is directly linked to the

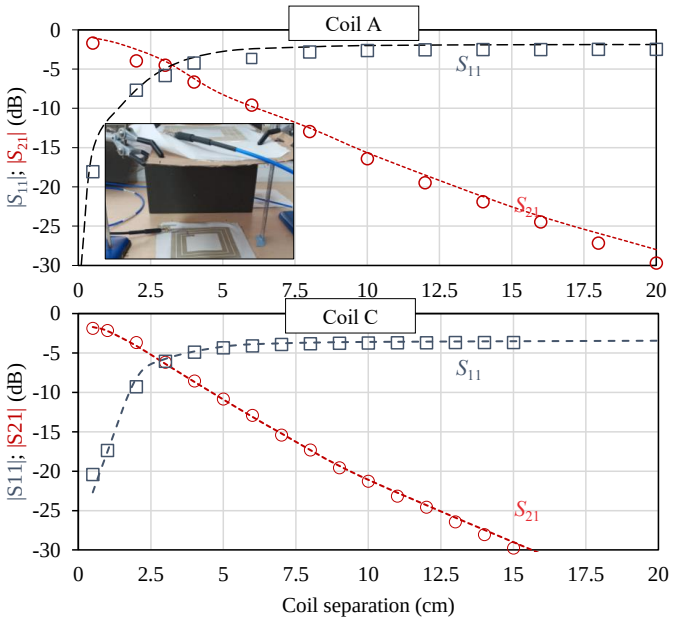

Fig. 6. Simulated (dashed line) and measured (solid markers) s-parameters of the symmetric link using coils A and C over varying distance; the inset shows the measurement setup.

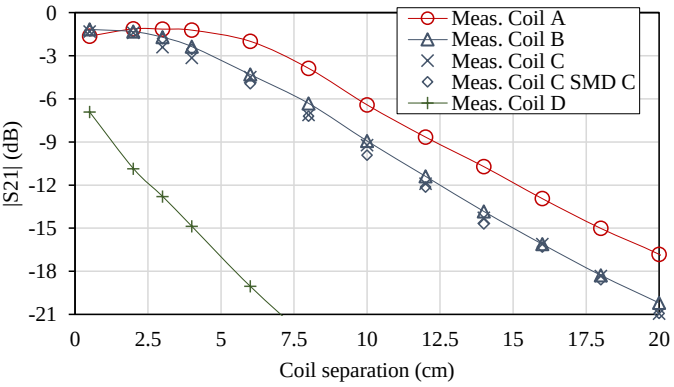

Fig. 7. Measured forward transmission between the textile coils and the reference wire transmitter over varying coil separations.

coil's radius, which is attributed to the effect of the gap on the mutual inductance [31]. Frequency-splitting and over-coupling [10] are not observed due to their relatively low Q-factor of the coils. The effect of lateral misalignment on the S_{21}, shown in Fig. 8, is directly related the coils' radii and the relative misalignment between the transmitting and receiving coil areas.

It is noted that the use of different coil geometries [32] or intermediate resonant coils or "meta-surfaces" can improve the link efficiency [11], [33]. However, the main focus of this work is to demonstrate a high-power WPT-enabled wearable system using all-printed passives, which to date has primarily been hindered by the rectifiers' or resonators' power handling as opposed to efficient resonator design.

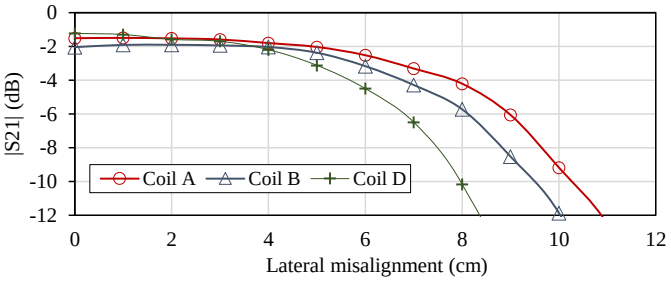

Fig. 8. Measured forward transmission between the textile coils and the reference wire transmitter over varying coil separations.

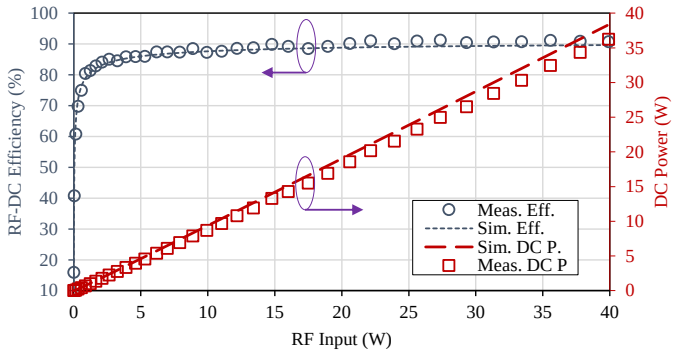

Fig. 9. Simulated and measured PCE and DC voltage output of the rectifier across a 261 Ω load.

IV. High-Power WPT Characterization

A. Rectifier Simulation and Measurements

The rectifier was simulated in Keysight ADS using harmonic balance simulation. The diode's parameters were taken from the datasheet and the 1 nF charge-pumping and smoothing capacitors were assumed to be ideal. A connectorized prototype of the proposed rectifier was fabricated for experimental validation. A load sweep was performed to identify the optimum load impedance Z_L in the >1 W power range; the rectifier maintains over 90% of its peak RF-DC efficiency for Z_L between 250 and 300 Ω. To characterize the rectifier under high power levels, the rectifier was connected directly to the 50 W PA demonstration kit's output and the PA's supply voltage was varied.

The input RF power was calculated using the PA's datasheet peak efficiency of 91% for a conservative estimate of the rectifier's performance. Fig. 9 shows the simulated and measured DC output and efficiency of the rectifier for varying RF inputs up to the PA's maximum output. Despite its flexible and low-cost implementation, the rectifier can generate up to 35 W DC output with an efficiency over 80% for inputs exceeding 1 W. This represents over 20× improvement over previously reported WPT rectifiers reported for wearable (Qi) applications [23] or operating at higher frequencies for near-field charging of textile-based devices [16].

B. Coil and System Characterization

The rectifier's layout was integrated with the MIM capacitor and the screen-printed coils on a single substrate, as seen in Fig. 1(b). Coil A (having the largest dimensions and

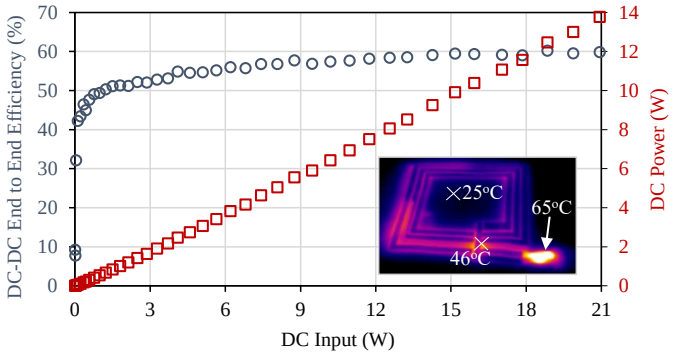

Fig. 10. Measured DC power output of a small gap (<0.5 cm) wireless gap and end-to-end DC-DC efficiency as a function of the DC input; the inset shows the temperature of the coil at maximum loading.

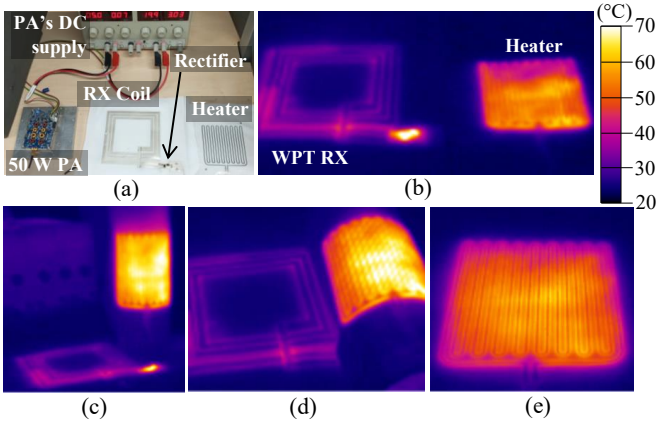

Fig. 11. The wireless-powered heater: (a) measurement setup; (b) IR image under flat conditions (<0.5 cm coil separation); (c, d) the functional heater under bending; (e) the heater powered with a 2 cm gap between the coils with a 3 W DC received power.

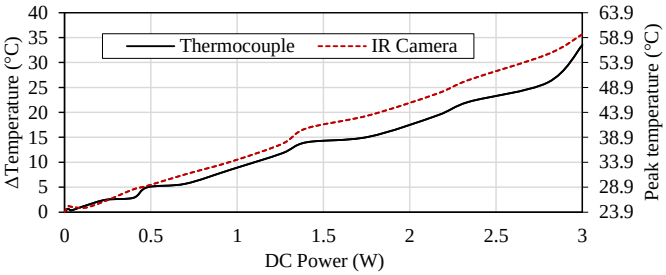

Fig. 12. Peak temperature of the screen-printed carbon/silver heater using a bench power supply.

Q-factor) was used to characterize the full WPT system. Two identical coils were used for transmitting and receiving, thereby enabling the power handling ability of the textile coil to be investigated.. The separation between the two coils has been kept under 5 mm, formed by the textile substrates and a non-uniform air gap due to the coils' flexibility. In this configuration, the coils maintained an S_{21}=−1.7 dB translating to a WPT link efficiency of 67%. Combined with the rectifier's efficiency of approximately 90% and the PA's DC-RF efficiency exceeding 91%, an end-to-end efficiency between 55% and 60% could be expected depending on the PA and rectifier's power-dependent performance.

To evaluate the system's power handling, the DC input to the PA was varied for a fixed coil separation of approximately 5 mm. Fig. 10 shows the measured end-to-end system efficiency and the DC power delivered to the load as a function of the DC input. A maximum DC input of 21 W was limited by the PA's current draw at maximum bias, which could be further increased through adaptive impedance matching or using multiple loads. However, as this work focuses on the coil, power conversion, and load implementation, such optimizations were not explored.

From Fig. 10, it can be seen that the maximum expected efficiency of 60% is approached for high input power levels, and that the end-to-end efficiency exceeds 50% for inputs exceeding 1.5 W. At its maximum DC power output of 14 W, a 60 V potential was measured across the 261 Ω 100 W-rated dummy load. To explore the coils' power handling, an infrared (IR) thermal camera (Testo 875i) was used to observe the temperature over the receiving coil.

The inset in Fig. 10 shows the peak temperatures measured over the receiving coil's surface while being driven at a 21 W DC input, where a maximum temperature rise of 21°C is observed over the coil, and around 40°C rise is recorded at the rectifier. The higher temperature increase over the rectifier's surface is attributed to the diodes' series resistance being confined to their very small footprint, resulting in lower heat dissipation. However, the proposed rectifier and tuning capacitor reduce the temperature rise over prior flexible rectifiers, which could not operate above 4 W due to the temperature rising above 180 °C [24].

C. Wireless-Powered Heater System Evaluation

A key example of thermal e-textiles are long-term therapeutics and recovery [14], [34], where a temperature up to 60°C could be required. The performance of the WPT system if further evaluated in conjunction with the load, the resistive printed heater. To realize the heater on the same fabric substrate, a 65%/35% carbon/silver paste was prepared and screen-printed onto a PU film which is then laminated on the same textile material alongside the coils. The carbon/silver formula was optimized to achieve a resistance as close as possible to the optimum load of the rectifier. The heater is formed of a meandered trace with 18 folds and is 9×9 cm. The cured and laminated heater had a measured low-voltage resistance of 270 Ω at room temperature. Fig. 11(a) shows the experimental setup used in evaluating the wireless-powered heater.

Prior to testing the integrated system, the heater was connected directly to a bench DC power supply to evaluate its power requirements. The IR camera was used to observe the thermal distribution over the heater and a thermocouple was placed where the highest temperatures were observed to cross-validate the IR measurements. Fig. 12 shows the heater's temperature change and absolute peak temperate as a function of its DC input up to 30 V. In most wearable rehabilitation and treatment applications, temperatures exceeding 60°C are not typically required [35]. Therefore, the maximum DC power

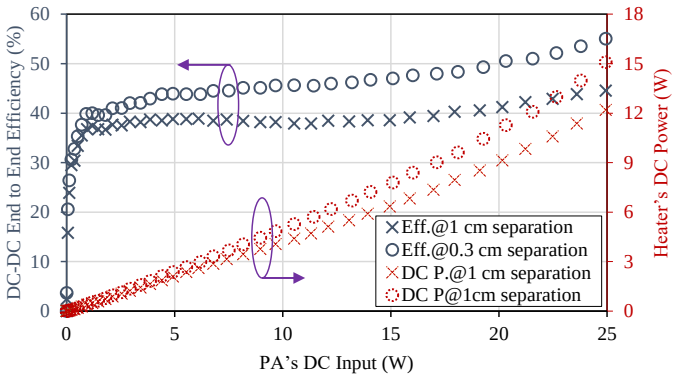

Fig. 13. The end-to-end efficiency and received power using the heater as a load for varying input power levels at different separations.

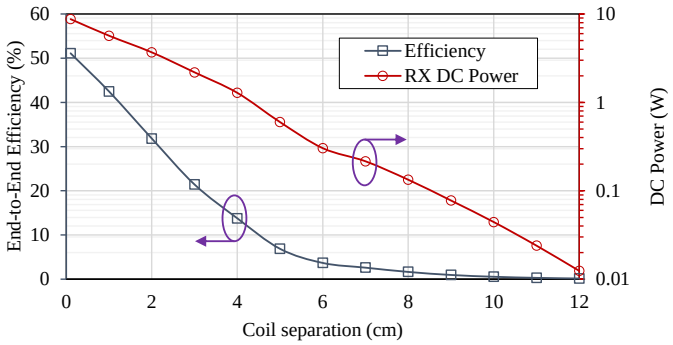

Fig. 14. Characterization of the DC power delivery to the heater over varying separation from the transmitter.

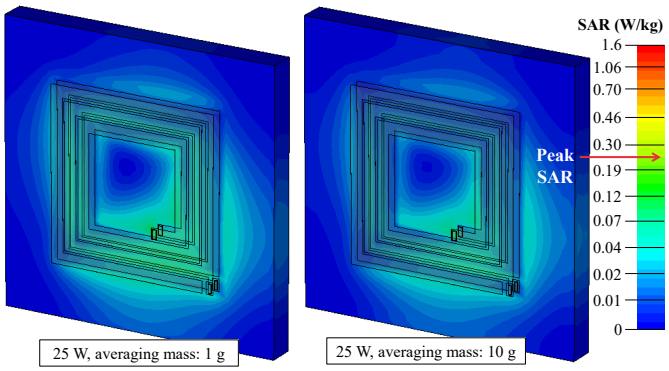

Fig. 15. Simulated SAR distribution for 25 W of 6.78 MHz power at the receiving (on-body) coil.

consumption of the heater can be estimated to be 3 W.

The heater was subsequently connected to the rectifier's output, as in Fig. 11(a), and a DC input power sweep was performed at two different separations between the transmitting and receiving textile coils. Low resistance conductive copper threads were used to connect the rectifier's DC output to the heater to demonstrate that the heater could be placed on a different body part to that hosting the coil. Fig. 13 shows the measured DC power delivered to the heater and the calculated end-to-end efficiency of the WPT system as it powers the load. The temperature of the wearable heater when driven at 15 W is shown in the IR photographs in Fig. 11(b) to (d), including when the heater is bent.

It can be observed in Fig. 13 that the peak end-to-end efficiency approaches that observed with the dummy resistive load. Moreover, a peak DC power output of 15 W could be delivered to the heating element. Given the maximum power consumption of 3 W for a peak temperature of 59°C to be reached by the heater, in Fig. 13, the received DC power is sufficient for powering multiple heating elements on different body parts. The control circuitry could also be powered within the available energy budget and a wearable energy storage device could also be charged [9].

Following the validation of the WPT-powered heating system and identifying 3 W as the peak power consumption of the individual heater, the system was characterized for varying coil separations. Fig. 14 shows the measured DC power output as a function of separation distance between the textile-based transmitter and receiver. At 2 cm separation, the DC power output is just over 3 W which can supply the heater with an end-to-end efficiency around 30%; this efficiency is comparable to that of a Qi-standard WPT system which can only deliver 1.2 W with minimal coil separation and using rigid power conversion circuitry of higher complexity [23].

In Fig. 11(e), the temperature across the surface of the heater with the 2 cm coil separation results in a peak temperature exceeding 60°C. At higher separation distances, the power output drops to mW levels which can only be used to power smaller sensors and wearable devices. Beyond 12 cm, the DC power output is comparable to that of radiative far-field WPT systems implying that a dual-mode near/far-field implementation could be utilized [17], [24].

The final step in characterizing the WPT system is evaluating its safety for use in a standard unregulated setting. The Specific Absorption Rate (SAR) was simulated over a homogeneous skin phantom placed with 1 mm separation from the receiving coil. The SAR was calculated in CST Microwave Studio and averaged over 10 and 1 g tissue mass. Fig. 15 shows the simulated SAR distribution, calculated for a 25 W input at the on-body receiving coil. With a peak SAR of 0.247 W/kg for a 25 W received RF power level, it can be seen that the coils operate well below the 1.6 W/kg SAR limit of the IEEE C95.1 standard. Therefore, the main limiting factor for the power level at which the coils can be driven at will be the heat dissipation of both the coils and rectifier, which could cause discomfort to the user.

Despite the extensive literature on electromagnetic near-field links for wearable WPT, there are limited works which have demonstrated a full system including the power conversion circuitry and a load. Table II compares this work to state-of-the-art wearable WPT receivers from the near-field to far-field. From Table II, it can be seen that the proposed system represents over a five-fold improvement in the DC power output over previous flexible WPT implementations and at least 100% DC-DC efficiency improvement, while being the first to use an all-flexible receiver. Moreover, the all-flexible screen-printed fabrication process enables the system to be scaled for most large-area industrial electronic applications. Finally, this work is the first to demonstrate a high-power wearable application, a textile-based Joule heater, being wirelessly-powered using

TABLE II
COMPARISON WITH RECENT WEARABLE WIRELESS POWER RECEIVERS

Work and WPT mode	DC Power	Peak Efficiency	Resonator/ antenna material	Rectifier materials
This work: IPT	1–15 W with >50% DC-DC efficiency	DC-DC: 60%; RF-DC: 90%	Printed silver on textile	Printed silver with SiC diodes
[23]: Qi IPT	1.51 W with <37% DC-DC efficiency	DC-DC: 37%; RF-DC: NR	Screen-printed coil	COTS Qi rectifier
[24]: 6.78 MHz resonant IPT	1–3.5 W with <32% DC-DC efficiency	DC-DC: 32%; RF-DC: ≈45%	Embroidered e-thread	Discrete capacitor with Si diodes
[16]: E/H mid-field coupling	1–200 mW	DC-DC: <5%; RF-DC: 50-80%	Embroidered e-thread	Discrete matching with Si diodes
[9]: far-field radiation	0.1–20 mW	DC-DC: <0.1%; RF-DC: 50-80%	Flexible circuit filament in textile	Discrete matching and diodes on a flex filament

NR: not reported, off-the-shelf rectifier

COTS parts with a high DC-DC efficiency approaching that of an ideal dummy load.

V. CONCLUSION

This paper presented an all-flexible printable WPT system and demonstrated it powering a textile-based Joule heater on the same substrate. The designed voltage doubler maintains an RF-DC efficiency over 80% for >1 W inputs, and a peak efficiency over 90% up to 40 W. The integrated system demonstrated a DC-DC efficiency approaching 60% with a 14 W DC output, enabling the textile-based heater to be powered at 2 cm away from the transmitter. The proposed system overcomes the limitations of existing flexible and wearable WPT systems based on:

1) High power handling: achieved through embedding a large-area low-loss tuning capacitor within the coil for improved thermal dissipation.
2) Reduced thermal losses: achieved through the use of low-loss diodes, reducing the temperature rise by nearly three-fold over previous flexible rectifiers.
3) Improved application-specific end-to-end efficiency, achieved by designing the load (the heating element) to approach the optimum current draw of the rectifier for improved RF-DC conversion.
4) Improved reliability and printability: by limiting the use of discrete rigid components to the SiC diodes as well as fabricating and encapsulating all passives using the same screen-printing process.

This work shows for the first time that flexible e-textile WPT systems can deliver Watt-level outputs efficiently. The printed heater demonstrated evidences that high-power wearable applications could become battery-free using WPT.

ACKNOWLEDGMENT

Datasets supporting this article will be made available from DOI: X.

REFERENCES

[1] B. Chu, W. Burnett *et al.*, "Bring on the bodyNET," *Nature*, vol. 549, p. 328â330, 2017.
[2] H.-T. Chang and J.-Y. Chang, "Sensor glove based on novel inertial sensor fusion control algorithm for 3-d real-time hand gestures measurements," *IEEE Transactions on Industrial Electronics*, vol. 67, DOI 10.1109/TIE.2019.2912765, no. 1, pp. 658–666, 2020.
[3] D. Patron, W. Mongan *et al.*, "On the use of knitted antennas and inductively coupled rfid tags for wearable applications," *IEEE Transactions on Biomedical Circuits and Systems*, vol. 10, DOI 10.1109/TBCAS.2016.2518871, no. 6, pp. 1047–1057, 2016.
[4] B.-J. Kim, Y. Jang *et al.*, "Self-powered carbon nanotube yarn for acceleration sensor application," *IEEE Transactions on Industrial Electronics*, vol. 68, DOI 10.1109/TIE.2020.2977541, no. 3, pp. 2676–2683, 2021.
[5] R. Pei, M. P. Leach *et al.*, "Wearable ebg-backed belt antenna for smart on-body applications," *IEEE Transactions on Industrial Informatics*, vol. 16, DOI 10.1109/TII.2020.2983064, no. 11, pp. 7177–7189, 2020.
[6] X. Tian, P. M. Lee *et al.*, "Wireless body sensor networks based on metamaterial textiles," *Nature Electronics*, vol. 2, pp. 243–251, 2019.
[7] L. Costanzo, M. Liu *et al.*, "Backpack energy harvesting system with maximum power point tracking capability," *IEEE Transactions on Industrial Electronics*, vol. 69, DOI 10.1109/TIE.2021.3053896, no. 1, pp. 506–516, 2022.
[8] A. Komolafe, B. Zaghari *et al.*, "E-textile technology reviewâfrom materials to application," *IEEE Access*, vol. 9, DOI 10.1109/ACCESS.2021.3094303, pp. 97 152–97 179, 2021.
[9] M. Wagih, N. Hillier *et al.*, "Rf-powered wearable energy harvesting and storage module based on e-textile coplanar waveguide rectenna and supercapacitor," *IEEE Open Journal of Antennas and Propagation*, vol. 2, DOI 10.1109/OJAP.2021.3059501, pp. 302 – 314, 2021.
[10] T. Imura and Y. Hori, "Maximizing air gap and efficiency of magnetic resonant coupling for wireless power transfer using equivalent circuit and neumann formula," *IEEE Transactions on Industrial Electronics*, vol. 58, no. 10, pp. 4746 – 4752, 2011.
[11] L. Li, H. Liu *et al.*, "Efficient wireless power transfer system integrating with metasurface for biological applications," *IEEE Transactions on Industrial Electronics*, vol. 65, DOI 10.1109/TIE.2017.2756580, no. 4, pp. 3230–3239, 2018.
[12] S. Lemey, F. Declercq, and H. Rogier, "Textile Antennas as Hybrid Energy-Harvesting Platforms," *Proc. IEEE*, vol. 102, no. 11, pp. 1833 – 1857, 2014.
[13] Z. Liu, P. Wu, and G. Li, "A multibeam and surface plasmonic clothing with rf energy-localized harvester for powering battery-free wireless sensor," *IEEE Internet of Things Journal*, vol. 9, DOI 10.1109/JIOT.2022.3142781, no. 15, pp. 13 955–13 964, 2022.
[14] Q. Liu, B. Tian *et al.*, "Recent advances in printed flexible heaters for portable and wearable thermal management," *Materials Horizons*, vol. 8, DOI 10.1039/D0MH01950J, no. 6, p. 1634â1656, Jun. 2021. [Online]. Available: https://pubs.rsc.org/en/content/articlelanding/2021/mh/d0mh01950j
[15] Y. Tang, L. Zhang *et al.*, "Multi-scale deep feature learning for human activity recognition using wearable sensors," *IEEE Transactions on Industrial Electronics*, DOI 10.1109/TIE.2022.3161812, pp. 1–1, 2022.
[16] D. Vital, P. Gaire *et al.*, "An ergonomic wireless charging system for integration with daily life activities," *IEEE Transactions on Microwave Theory and Techniques*, vol. 69, DOI 10.1109/TMTT.2020.3029530, no. 1, p. 947â954, Jan. 2021.
[17] M. Wagih, A. Komolafe *et al.*, "Broadband compact substrate-independent textile wearable antenna for simultaneous near- and far-field wireless power transmission," *IEEE Open Journal of Antennas and Propagation*, vol. 3, DOI 10.1109/OJAP.2022.3167089, pp. 398–411, 2022.
[18] S. H. Kang and C. W. Jung, "Textile Resonators With Thin Copper Wire for Wearable MR-WPT System, year=2017," *IEEE Microwave and Wireless Components Letters*, vol. 27, DOI 10.1109/LMWC.2016.2629976, no. 1, pp. 91–93.
[19] S. H. Kang, V. T. Nguyen, and C. W. Jung, "Analysis of mrâwpt using planar textile resonators for wearable applications," *IET Microwaves, Antennas & Propagation*, vol. 10, DOI 10.1049/iet-map.2016.0024, no. 14, p. 1541â1546, Nov. 2016. [Online]. Available: https://onlinelibrary.wiley.com/doi/10.1049/iet-map.2016.0024

[20] M. Wagih, A. Komolafe, and B. Zaghari, "Dual-Receiver Wearable 6.78 MHz Resonant Inductive Wireless Power Transfer Glove Using Embroidered Textile Coils," *IEEE Access*, vol. 8, pp. 24 630 – 24 642, 2020.

[21] A. E. Ostfeld, I. Deckman *et al.*, "Screen printed passive components for flexible power electronics," *Sci. Rep.*, vol. 5, DOI 10.1038/srep15959, p. 15959, 2015.

[22] M. Wagih, A. Komolafe, and N. Hillier, "Screen-printable flexible textile-based ultra-broadband millimeter-wave dc-blocking transmission lines based on microstrip-embedded printed capacitors," *IEEE Journal of Microwaves*, vol. 2, DOI 10.1109/JMW.2021.3126927, no. 1, pp. 162–173, 2022.

[23] Y. Li, N. Grabham *et al.*, "Textile-Based Flexible Coils for Wireless Inductive Power Transmission," *Applied Sciences*, vol. 8, DOI 10.3390/app8060912, no. 6, 2018.

[24] M. Wagih, A. Komolafe *et al.*, "1 µw-3.75 w dual-mode near/far-field wearable wireless power transfer using a hybrid rectenna," in *2022 Wireless Power Week (WPW)*, DOI 10.1109/WPW54272.2022.9853859, pp. 298–301, 2022.

[25] K. Yang, K. Meadmore *et al.*, "Development of user-friendly wearable electronic textiles for healthcare applications," *Sensors*, vol. 18, DOI 10.3390/s18082410, no. 8, 2018. [Online]. Available: https://www.mdpi.com/1424-8220/18/8/2410

[26] K. Yang, R. Torah *et al.*, "Waterproof and durable screen printed silver conductive tracks on textiles," *Textile Research Journal*, vol. 83, pp. 2023 – 2031, 2013.

[27] B. S. Cook, J. R. Cooper, and M. M. Tentzeris, "Multi-layer rf capacitors on flexible substrates utilizing inkjet printed dielectric polymers," *IEEE Microwave and Wireless Components Letters*, vol. 23, DOI 10.1109/LMWC.2013.2264658, no. 7, pp. 353–355, 2013.

[28] S. Mohan, M. del Mar Hershenson *et al.*, "Simple accurate expressions for planar spiral inductances," *IEEE Journal of Solid-State Circuits*, vol. 34, DOI 10.1109/4.792620, no. 10, pp. 1419–1424, 1999.

[29] K. Pan, Y. Fan *et al.*, "Sustainable production of highly conductive multilayer graphene ink for wireless connectivity and iot applications," *Nature Communications*, vol. 9, DOI 10.1038/s41467-018-07632-w, no. 1, p. 5197, Dec. 2018. [Online]. Available: https://www.nature.com/articles/s41467-018-07632-w

[30] B. S. Cook, C. Mariotti *et al.*, "Inkjet-printed, vertically-integrated, high-performance inductors and transformers on flexible LCP substrate," in *2014 IEEE MTT-S International Microwave Symposium (IMS2014)*, DOI 10.1109/MWSYM.2014.6848575, pp. 1–4, 2014.

[31] S. Raju, R. Wu *et al.*, "Modeling of mutual coupling between planar inductors in wireless power applications," *IEEE Transactions on Power Electronics*, vol. 29, no. 1, pp. 481 – 490, 2014.

[32] M. R. Basar, M. Y. Ahmad *et al.*, "An improved wearable resonant wireless power transfer system for biomedical capsule endoscope," *IEEE Transactions on Industrial Electronics*, vol. 65, DOI 10.1109/TIE.2018.2801781, no. 10, pp. 7772–7781, 2018.

[33] S.-J. Huang, T.-S. Lee *et al.*, "Intermediate coil-aided wireless charging via interactive power transmitting with misalignment-tolerating considerations," *IEEE Transactions on Industrial Electronics*, vol. 69, DOI 10.1109/TIE.2021.3123665, no. 10, pp. 9972–9983, 2022.

[34] J. T. Selsby and S. L. Dodd, "Heat treatment reduces oxidative stress and protects muscle mass during immobilization," *American Journal of Physiology-Regulatory, Integrative and Comparative Physiology*, vol. 289, DOI 10.1152/ajpregu.00497.2004, no. 1, p. R134âR139, Jul. 2005. [Online]. Available: https://journals.physiology.org/doi/full/10.1152/ajpregu.00497.2004

[35] H. McGorm, L. A. Roberts *et al.*, "Turning up the heat: An evaluation of the evidence for heating to promote exercise recovery, muscle rehabilitation and adaptation," *Sports Medicine*, vol. 48, DOI 10.1007/s40279-018-0876-6, no. 6, p. 1311â1328, Jun. 2018. [Online]. Available: https://doi.org/10.1007/s40279-018-0876-6

Mahmoud Wagih (GS'18, M'21) received his B.Eng. (Hons.) in September 2018, and his Ph.D. on rectenna design in April 2021, both in Electrical and Electronic Engineering from the University of Southampton.

He is a currently a UK IC Research Fellow and Proleptic Lecturer (Assistant Professor) with the James Watt School of Engineering at the University of Glasgow. His interests broadly cover antennas and microwave systems for energy harvesting, sensing, and wearable applications.

Dr. Wagih was the recipient of several prizes including the Best in Engineering and Physical Sciences Doctoral Research Award, Best in Faculty Doctoral Research Award, in 2018-2021, at the University of Southampton. He received the Best Student Paper Award at the IEEE Wireless Power Transfer Conference, 2019, the Best Oral Presentation at PowerMEMS, 2019, the Best Paper Award at PowerMEMS, 2021, the IEEE MTT-S Best 3MT Presentation Prize (second place) at the IEEE Microwave Week, 2020, was a U.K. TechWorks Young Engineer of the Year finalist, in 2021, received the EurAAP Per-Simon Kildal Award for the Best PhD in Antennas and Propagation, and an International Union of Radio Science (URSI) Young Scientist Award, in 2022. He is a Senior Member of URSI, and is an affiliate member of the IEEE Microwave Theory & Technologies Technical Committees TC-25, on Wireless Power, and TC-26, on RFID/IoT.

Abiodun Komolafe received the B.Sc. degree (Hons.) in physics from the University of Ibadan, Nigeria, in 2007, the M.Sc. degree in microelectromechanical systems, in 2011, and the Ph.D. degree in printed circuits on fabrics from the University of Southampton, in 2016.

He currently works as a Research Fellow with the University of Southampton in investigating novel manufacturing methods for making functional electronics on textiles using flexible electronic circuits and screen-printed electronics for medical applications. He is experienced in the design and fabrication of e-textiles using screen printing and thin-film technologies

Alex S. Weddell (GS'06-M'10) received the M.Eng. degree (1st class honors) and Ph.D. in electronic engineering from the University of Southampton, U.K., in 2005 and 2010.

His main research focus is in the areas of energy harvesting and energy management for future Internet of Things devices. He has over 14 yearsâ experience in design and deployment of energy harvesting systems.He is currently a Lecturer in the Center for Internet of Things and Pervasive Systems at the University of Southampton, and is involved with three projects funded by EPSRC, EU Horizon 2020 and Clean Sky 2.

Steve Beeby (FIEEE) received the B.Eng. (Hons.) degree in mechanical engineering from the University of Portsmouth, Portsmouth, U.K., in 1992, and the Ph.D. degree in MEMS resonant sensors from the University of Southampton, Southampton, U.K., in 1998.

He is currently the Director of the Centre for Flexible Electronics and E-Textiles at the University of Southampton, and leads the U.K.'s E-Textiles Network. He is has received over £20 million research funding. He is a co-founder of Perpetuum Ltd., a University spin-out based upon vibration energy harvesting formed in 2004, Smart Fabric Inks Ltd., and D4 Technology Ltd. He has given over 30 plenary/keynote/invited talks and has over 350 publications and an h-Index of 59. His current research interests focus on energy harvesting, e-textiles and the use of energy harvesting in wearable applications.

Prof. Beeby was the recipient of two prestigious EPSRC Research Fellowships to investigate the combination of screen-printed active materials with micromachined structures and textiles for energy harvesting. He has most recently been awarded a prestigious RAEng Chair in Emerging Technologies in E-textile Engineering.